

Reaction cross section described by a black sphere approximation of nuclei

Akihisa Kohama,¹ Kei Iida,^{1,2} and Kazuhiro Oyamatsu^{1,3,4}

¹RIKEN (The Institute of Physical and Chemical Research),

2-1 Hirosawa, Wako-shi, Saitama 351-0198, Japan

²RIKEN BNL Research Center, Brookhaven National Laboratory, Upton, New York 11973-5000

³Department of Media Theories and Production, Aichi Shukutoku University,

Nagakute, Nagakute-cho, Aichi-gun, Aichi 480-1197, Japan

⁴Department of Physics, Nagoya University, Furo-cho, Chigusa-ku, Nagoya, Aichi 464-8602, Japan

(Dated: December 17, 2018)

We identify a length scale that simultaneously accounts for the observed proton-nucleus reaction cross section and diffraction peak in the proton elastic differential cross section. This scale is the nuclear radius, a , deduced from proton elastic scattering data of incident energies higher than ~ 800 MeV, by assuming that the target nucleus is a “black” sphere. The values of a are determined so as to reproduce the angle of the first diffraction maximum in the scattering data for stable nuclei. We find that the absorption cross section, πa^2 , agrees with the empirical total reaction cross section for C, Sn, and Pb to within error bars. This agreement persists in the case of the interaction cross section measured for a carbon target. We also find that $\sqrt{3/5}a$ systematically deviates from the empirically deduced values of the root-mean-square matter radius for nuclei having mass less than about 50, while it almost completely agrees with the deduced values for $A \gtrsim 50$. This tendency suggests a significant change of the nuclear matter distribution from a rectangular one for $A \lesssim 50$, which is consistent with the behavior of the empirical charge distribution.

PACS numbers: 25.60.Dz, 21.10.Gv, 24.10.Ht, 25.40.Cm

The size of atomic nuclei is considered to be well deduced from empirical data for the proton-nucleus elastic differential cross section, $d\sigma_{\text{el}}/d\Omega$, and the total reaction cross section, $\sigma_R \equiv \sigma_T - \sigma_{\text{el}}$, where σ_T is the total cross section. So far, the analysis that respects both data in deducing the nuclear size has not been completed in particular for proton incident energies, T_p , higher than 800 MeV. Various approximate theories based on optical potentials have been proposed to reproduce the elastic scattering data, while they usually tend to overestimate the reaction cross section for 800 MeV $\lesssim T_p \lesssim 1000$ MeV (e.g., Ref. [1] and references therein).

In Ref. [2], we constructed a method for deducing the nuclear size by focusing on the peak angle in the proton-nucleus elastic differential cross section measured at $T_p \gtrsim 800$ MeV, where the corresponding optical potential is strongly absorptive. In this method, we regard a nucleus as a “black” (i.e., purely absorptive) sphere of radius a , and determine a in such a way as to reproduce the angle of the observed first diffraction peak. If we multiply a by $\sqrt{3/5}$, a ratio between the root-mean-square and squared off radii for a rectangular distribution, the result for stable nuclei of $A \gtrsim 50$ shows an excellent agreement with the root-mean-square radius, r_m , of the matter density distribution as determined from conventional scattering theories so as to reproduce the overall diffraction pattern and analyzing power in the proton elastic scattering.

In this paper, we extend such a previous analysis to the case of $A \lesssim 50$, and find out a systematic deviation between $\sqrt{3/5}a$ and r_m . We next show that the present method is effective at explaining the observed re-

action cross sections for stable nuclei ranging from light to heavy ones. In the black sphere approximation of a nucleus, where the geometrical cross section can be described by πa^2 , a plays the role of a critical radius inside which the reaction with incident protons occurs. We find that πa^2 is consistent with the measured reaction cross section. Consequently, the black sphere picture characterized by a gives a unified basis for describing the reaction cross section and the elastic scattering data. This simple formula for the reaction cross section, given by πa^2 , does not include any adjustable parameter. This is a feature more advantageous than the fitting formulas proposed earlier [3, 4] on the basis of the $A^{1/3}$ law.

We start with evaluations of a for stable nuclei including light elements by following a line of argument of Ref. [2]. The center-of-mass (c.m.) scattering angle for proton elastic scattering is generally given by $\theta_{\text{c.m.}} = 2 \sin^{-1}(q/2p)$ with the momentum transfer, \mathbf{q} , and the proton incident momentum in the c.m. frame, \mathbf{p} . For the proton diffraction by a circular black disk of radius a , we can calculate the value of $\theta_{\text{c.m.}}$ at the first peak as a function of a . (Here we define the zeroth peak as that whose angle corresponds to $\theta_{\text{c.m.}} = 0$.) We determine a in such a way that this value of $\theta_{\text{c.m.}}$ agrees with the first peak angle for the measured diffraction in proton-nucleus elastic scattering, θ_M . The radius, a , and the angle, θ_M , are then related by

$$2pa \sin(\theta_M/2) = 5.1356 \dots \quad (1)$$

By setting

$$r_{\text{BS}} \equiv \sqrt{3/5}a, \quad (2)$$

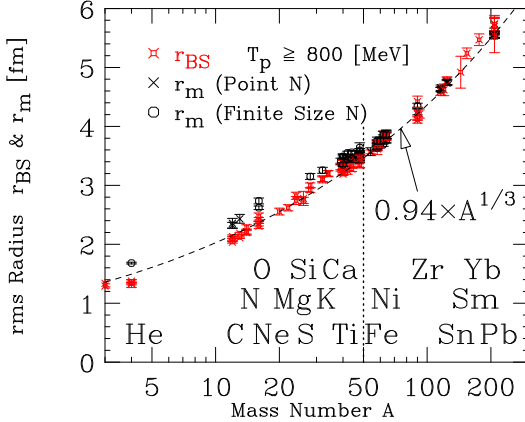


FIG. 1: (Color) r_{BS} as a function of mass number, A . For nuclei of $A > 50$, we have plotted the values of r_m adopted in Ref. [2]. For the error bars in r_{BS} and r_m , see Ref. [2]. For comparison we also plot the results for r_m derived in the following references: For ^{12}C , in Refs. [5, 6, 7] ($T_p = 800$ MeV); for ^{13}C , in Refs. [5, 7] ($T_p = 800$ MeV); for ^{16}O , in Refs. [8, 9] ($T_p = 1000$ MeV); for ^{28}Si , in Ref. [8] ($T_p = 1000$ MeV); for ^{32}S , in Ref. [8] ($T_p = 1000$ MeV); for ^{39}K , in Ref. [8] ($T_p = 1000$ MeV); for $^{40,48}\text{Ca}$, in Ref. [10] ($T_p = 796$ MeV), in Ref. [8] ($T_p = 1000$ MeV); for $^{40,42,44,48}\text{Ca}$, in Ref. [11] ($T_p = 796$ MeV), in Refs. [9, 12] ($T_p = 1044$ MeV); for $^{46,48}\text{Ti}$, in Ref. [13] ($T_p = 799.3$ MeV); for ^{48}Ti , in Ref. [12] ($T_p = 1044$ MeV). For ^4He , the root-mean-square radius of the charge density distribution deduced from electron elastic scattering data [14, 15] is plotted instead of r_m , because no r_m is available for this case. The crosses (\times) denote the root-mean-square matter radii of the point nucleon distributions, and the circles (\circ) denote those folded with the nucleon form factor. The dashed curve represents $0.94A^{1/3}$ fm. The dotted line shows $A = 50$.

we found [2] that at $T_p \gtrsim 800$ MeV, r_{BS} , estimated for heavy stable nuclei of $A > 50$, is within error bars consistent with the root-mean-square nuclear matter radius, r_m , deduced from elaborate analyses based on conventional scattering theory. Thus, expression (2) works as a “radius formula.” The factor $\sqrt{3/5}$ comes from the assumption that the nucleon distribution is rectangular; the root-mean-square radius of a rectangular distribution is a cutoff radius multiplied by $\sqrt{3/5}$. Here we simply extend this estimate of r_{BS} to lighter stable nuclei. This extension of the black sphere analysis is reasonable as long as the scattering is close to the limit of the geometrical optics. This condition is fairly well satisfied at least for $T_p \gtrsim 800$ MeV, since a/λ , where $\lambda = 2\pi/p$ is the wave length of incident proton in the c.m. frame, is well above unity even for ^4He . As we shall see, the values of r_{BS} are systematically smaller than those of r_m for $A < 50$, whereas the values of πa^2 for C, Sn, and Pb agree well with the proton-nucleus reaction cross section data for $T_p \gtrsim 800$ MeV.

The values of r_{BS} , which are obtained for stable nuclei ranging from He to Pb from the proton elastic scat-

tering data for $T_p \gtrsim 800$ MeV, are plotted in Fig. 1, together with the values of r_m estimated in earlier investigations. In collecting the data, we have made access to Experimental Nuclear Reaction Data File (EXFOR) [16]. In deriving r_{BS} for ^3He , we have used the data for $T_p = 800$ MeV [17] and for $T_p = 1040$ MeV [18]. Since the peak position is not clear, we do not include the data for $T_p = 1000$ MeV [19] in this analysis. For ^4He , we have used the data for $T_p = 1000$ MeV [20, 21], $T_p = 1050$ MeV [22], and $T_p = 1150$ MeV [23]. We remark that, for $T_p = 890, 991$ MeV, no peak has been identified since the measured cross sections are limited to very forward direction [24]. For C and heavier isotopes, we have used the following data: ^{12}C ($T_p = 800$ MeV) [6, 7, 25]; ^{13}C ($T_p = 800$ MeV) [6, 7, 26]; ^{12}C ($T_p = 1000$ MeV) [27]; ^{12}C ($T_p = 1040$ MeV) [28]; ^{14}N ($T_p = 800$ MeV) [26, 29]; ^{14}N ($T_p = 1000$ MeV) [30]; ^{16}O ($T_p = 800$ MeV) [31, 32]; ^{16}O ($T_p = 1000$ MeV) [30, 33]; ^{20}Ne ($T_p = 800$ MeV) [34]; ^{22}Ne ($T_p = 800$ MeV) [35]; ^{24}Mg ($T_p = 800$ MeV) [36, 37, 38]; ^{26}Mg ($T_p = 800$ MeV) [37, 38]; ^{28}Si ($T_p = 1000$ MeV) [8, 39]; $^{32,34}\text{S}$ ($T_p = 1000$ MeV) [30, 39]; ^{39}K ($T_p = 1000$ MeV) [30, 40]; $^{40,42,44,48}\text{Ca}$ ($T_p = 796$ MeV) [11]; ^{40}Ca ($T_p = 797.5$ MeV) [41]; ^{40}Ca ($T_p = 800$ MeV) [32, 42]; ^{40}Ca ($T_p = 1000$ MeV) [30, 40]; ^{40}Ca ($T_p = 1044$ MeV) [12]; $^{42,44}\text{Ca}$ ($T_p = 800$ MeV) [42]; $^{42,44}\text{Ca}$ ($T_p = 1044$ MeV) [12]; ^{48}Ca ($T_p = 800$ MeV) [42]; ^{48}Ca ($T_p = 1000$ MeV) [30]; ^{48}Ca ($T_p = 1044$ MeV) [12]; $^{46,48}\text{Ti}$ ($T_p = 799.3$ MeV) [13]; ^{48}Ti ($T_p = 1044$ MeV) [12]. We do not include the data for ^9Be ($T_p = 1000$ MeV) [43], ^{12}C ($T_p = 1000$ MeV) [20], nor ^{16}O ($T_p = 1000$ MeV) [20] since the peak positions are not clear.

It is interesting to note that r_{BS} agrees almost completely with r_m for $A > 50$, as shown in Ref. [2], while it is smaller than r_m by about 0.2 fm for $A < 50$. In order to clarify this deviation, we exhibit the difference, $r_{BS} - r_m$, in Fig. 2. The drastic change in the difference around $A \sim 50$ implies a possible change in the form of the real nucleon distribution; the rectangular distribution as assumed in the present black sphere model may well simulate the real distribution at $A > 50$, while for $A < 50$ the real distribution is quite different from the rectangular one in such a way that the portion of the real distribution farther than a is relatively large. This feature is suggested by the empirical charge distribution deduced from the electron-nucleus elastic scattering [14], which shows a Gaussian-like form rather than a rectangular one for light nuclei.

This feature of the nucleon distribution is expected to be reflected by size-sensitive observables for which empirical data are available for stable nuclei ranging from light to heavy ones. Such observables include $1s$ states of pionic atoms and isoscalar giant resonance energies; the isoscalar part of the pion-nucleus optical potential [44] and the inertia associated with the resonances [45] are related to the nucleon distribution.

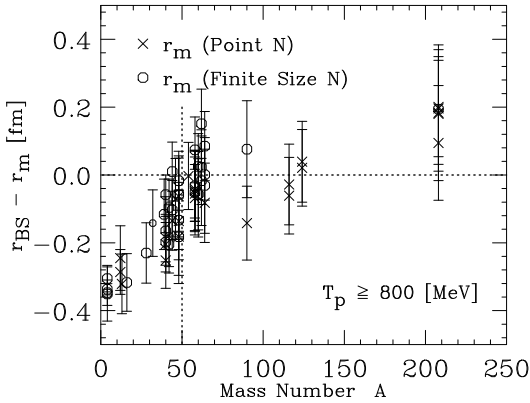


FIG. 2: The difference, $r_{BS} - r_m$, as a function of mass number, A . The crosses (\times) and the circles (\circ) are calculated from the corresponding values of r_m in Fig. 1. The dotted line shows $r_{BS} = r_m$ and $A = 50$.

We can see from Fig. 1 that r_{BS} , if having its staggering smoothed out, behaves as $\sim 0.94A^{1/3}$ fm. This suggests that r_{BS} and hence a provides a measure of the reaction cross section, since the empirical values are known to behave roughly as $\propto A^{2/3}$ [46]. It is thus interesting to compare the black sphere cross section with the empirical data.

We proceed to calculate the proton-nucleus total reaction cross section from the present black sphere model. Our model regards it as the geometrical cross section,

$$\sigma_{BS} \equiv \pi a^2. \quad (3)$$

Here we assume that the incident protons are point particles, and that the incident protons, if touching the target point nucleon distribution, contribute to the reaction cross section by yielding excitations associated with internucleon motion. Our model thus predicts vanishing cross section for the proton-proton case. This is reasonable since the proton-nucleon reaction cross section is relatively small for $T_p \lesssim 1$ GeV [47, 48].

By substituting the values of a determined by Eq. (1) into Eq. (3), we evaluate σ_{BS} for stable nuclei. In Fig. 3, the results are plotted together with the empirical data on σ_R available for $800 \text{ MeV} < T_p < 1000 \text{ MeV}$ [46]. We can see an excellent agreement between σ_{BS} and the empirical values although the comparison is possible only for C, Sn, and Pb. For these nuclei, as shown in Table I, σ_{BS} and σ_R agree with each other within the error bars. Note that we do not use any adjustable parameter here. We thus see the role played by σ_{BS} in predicting σ_R , and this is useful for nuclides for which elastic scattering data are available but no data for σ_R are available. On the other hand, if σ_R is measured, one can deduce a from Eq. (3). In this case, a can be regarded as a “reaction radius,” inside which the reaction with incident protons occurs. In a real nucleus, this radius corresponds to a radius at which the mean-free path of incident protons is

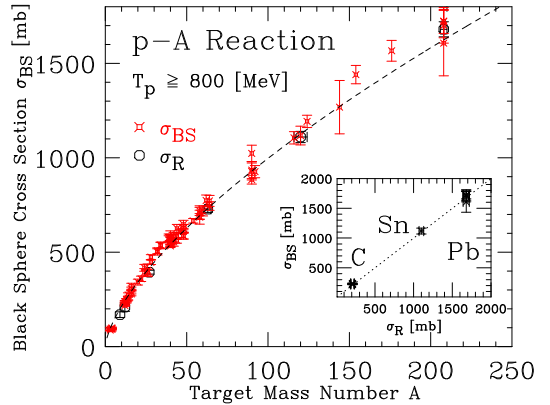


FIG. 3: (Color) The absorption cross section, σ_{BS} , of a proton of $T_p \gtrsim 800$ MeV by a target nucleus of mass number A . For comparison, we plot the empirical data for the proton-nucleus total reaction cross section, σ_R (\circ), which are listed in Ref. [46] for ^9Be , ^{27}Al , C, Cu, Sn, and Pb. For the latter four elements the value of σ_R is the average over the isotopic abundance in a target. For these data, we set A as the mass number of the most abundant isotope and assign the uncertainty in A due to the natural abundance. The dashed curve denotes $(5/3)\pi(0.94A^{1/3})^2$ fm 2 . Inset: σ_{BS} vs σ_R for C, Sn, and Pb. The dotted line represents $\sigma_{BS} = \sigma_R$.

of the order of the length of the penetration.

It is natural to generalize the definition of σ_{BS} given by Eq. (3) to the case of the nucleus-nucleus reaction cross section. We simply set

$$\sigma_{BS} = \pi(a_1 + a_2)^2, \quad (4)$$

where $a_1(a_2)$ is the black sphere radius of a projectile (target) nucleus, which we determine from the proton elastic differential cross section data for $T_p \gtrsim 800$ MeV.

In the case of nucleus-nucleus collisions, rather than to measure the reaction cross section σ_R , it is more convenient to measure the interaction cross section, $\sigma_I \equiv$

TABLE I: Values of σ_R and σ_{BS} for C, Sn, and Pb. The values of σ_R [46] are for natural targets, while those of σ_{BS} are for ^{12}C , ^{120}Sn , and ^{208}Pb , the elastic scattering data for which are taken from the references shown in the last column.

Target	σ_R [mb] (T_p [MeV])	σ_{BS} [mb] (T_p [MeV])	Ref.
C	209 ± 22 (860)	217.003 ± 3.45 (800)	[6]
		227.788 ± 3.46 (800)	[25]
		228.233 ± 9.20 (1000)	[27]
		237.562 ± 6.69 (1040)	[28]
Sn	1100 ± 30 (860)	1117.486 ± 49.6 (800)	[49]
Pb	1680 ± 40 (860)	1723.590 ± 88.5 (800)	[6]
		1721.680 ± 63.6 (800)	[50]
		1606.919 ± 173.0 (800)	[49]
		1701.161 ± 94.1 (1000)	[30]

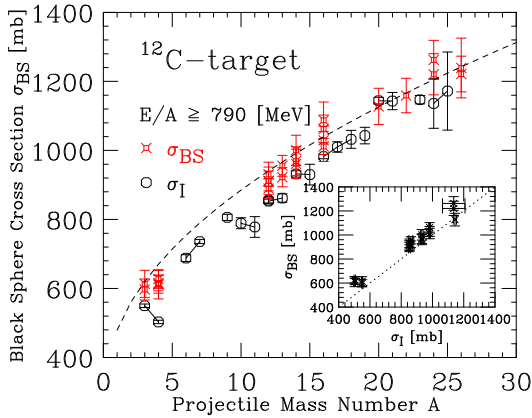


FIG. 4: (Color online) The absorption cross section σ_{BS} for a projectile stable nucleus of $A < 30$ and a ^{12}C target. We fix $r_{BS} = 2.086 \pm 0.05$ fm for ^{12}C . For comparison, we plot the interaction cross section, σ_I (○), measured at $E/A \gtrsim 800$ MeV for a projectile of $^{3,4}\text{He}$, $^{6,7}\text{Li}$, ^{9}Be , $^{10,11}\text{B}$, $^{12,13}\text{C}$, $^{14,15}\text{N}$, $^{16,17,18}\text{O}$, ^{19}F , $^{20,21}\text{Ne}$, ^{23}Na , and $^{24,25}\text{Mg}$ incident on a ^{12}C target [51]. The dashed curve represents $(5/3)\pi(2.086 + 0.94A^{1/3})^2 \text{ fm}^2$. Inset: σ_{BS} vs σ_I for ^4He , $^{12,13}\text{C}$, ^{14}N , ^{16}O , ^{20}Ne , and ^{24}Mg . The dotted line represents $\sigma_{BS} = \sigma_I$.

$\sigma_R - \sigma_{\text{inelab}}$, where σ_{inelab} is the cross section for inelastic channels. It is interesting to compare the measured values of σ_I with the corresponding values of σ_{BS} given by Eq. (4). The results are given in Fig. 4, together with the empirical data on σ_I measured with a ^{12}C target for stable nuclei of $E/A \gtrsim 800$ MeV [51].

We find from Fig. 4 that σ_{BS} agrees within error bars with the empirical values of σ_I except for a few cases. This result reassures the role played by the black sphere radius as a reaction radius. We also note the tendency that σ_{BS} is larger than σ_I . This is consistent with the facts that $\sigma_R > \sigma_I$ and that, for a ^{12}C projectile, σ_{BS} is much closer to the empirical value of σ_R [52] than that of σ_I .

It is also interesting to evaluate σ_{BS} for highly neutron-enriched nuclei once the proton elastic differential cross section is measured at high incident energies. If the proton reaction cross section σ_R or the interaction cross section σ_I is measured simultaneously, one could compare the result with σ_{BS} . If σ_{BS} is significantly smaller than σ_R (I), it would suggest that the significant contribution to σ_R (I) comes from the tail region farther than a . This could imply the possible presence of a neutron halo [51]. The comparison between σ_{BS} and σ_R (I) provides an important check of the widely accepted speculation that one can deduce the halo structure from measurements of the interaction cross section [53].

In summary we have extended our previous analysis of the nuclear size for $A > 50$ [2], which is based on the black sphere assumption of a nucleus, to lighter stable nuclei. The black sphere radius, a , has been determined

so as to reproduce the angle of the first diffraction maximum in the proton elastic scattering data. We have thus finalized a systematic analysis of the existing data for proton elastic scattering off stable nuclei ranging from He to Pb at proton incident energies above ~ 800 MeV. We have two significant results. First, the values of r_{BS} obtained from Eq. (2) are systematically larger than the root-mean-square radius r_m deduced from elaborate scattering theory for $A < 50$, although they agree quite well with each other for $A > 50$. This suggests a significant deviation of the nucleon distribution from the rectangular one for $A < 50$. Second, the absorption cross section, πa^2 , is consistent with the empirical total reaction cross section for C, Sn, and Pb. This consistency persists in the case of the interaction cross section measured for a carbon target. We thus see the dual role of a as a black sphere radius and as a reaction radius.

Elastic scattering and total reaction cross section data for heavy unstable nuclei are expected to be provided by radioactive ion beam facilities, such as GSI, Darmstadt, and the Radioactive Ion Beam Factory in RIKEN. Experiments at RIKEN are planned for a beam energy of a few hundreds MeV per nucleon. It is thus important to study the energy dependence of the black sphere radius, a . As a first trial, we have studied the case of ^{208}Pb , for which not only the de Broglie wavelength of the incident proton but also the mean-free path of the proton in the nuclear interior is sufficiently short compared to the nuclear radius, and confirmed that the resultant σ_{BS} agrees with the measured value of σ_R within the error bars for the proton incident energy down to a few hundreds MeV. The energy dependence is found to be similar to that of the nucleon-nucleon total cross section. This is consistent with the fact that the black sphere radius corresponds to the reaction radius. We remark that the energy dependence of a may well modify the relation between a and r_m [54].

Towards future possible application of the black sphere model to neutron-rich unstable nuclei, we here give a couple of examples, $^{6,8}\text{He}$ and ^{11}Li , for which empirical information on the proton-nucleus total reaction cross section is available at relatively high energy. Hereafter we will estimate the black sphere radius a from $\sigma_R = \pi a^2$ in the absence of the data for the first peak in the elastic diffraction pattern. From the empirical data, $\sigma_R = 161.3 \pm 3.7$ mb for ^6He ($E/A = 721$ MeV) and $\sigma_R = 197.8 \pm 3.5$ mb for ^8He ($E/A = 678$ MeV), measured by Neumaier *et al.* [55], we estimate $a = 2.27 \pm 0.03$ fm and $r_{BS} = 1.76 \pm 0.03$ fm for ^6He , and $a = 2.51 \pm 0.02$ fm and $r_{BS} = 1.94 \pm 0.02$ fm for ^8He . The values of r_m deduced from the elastic scattering data [56] are $r_m = 2.45 \pm 0.10$ fm for ^6He and $r_m = 2.53 \pm 0.08$ fm for ^8He . We thus see a difference between r_m and r_{BS} of order 0.7 fm, which is significantly larger than that for light stable nuclei (see Fig. 2.) For ^{11}Li , we take note of the data for the interaction cross section obtained for a proton target: $\sigma_I = 276 \pm 8$ mb

at 800 MeV/A [57]. If we assume $\sigma_R = \sigma_I$, we obtain $a = 2.96 \pm 0.04$ fm and $r_{BS} = 2.30 \pm 0.04$ fm. Since the typical value of r_m amounts to about 3.1 fm [51], we obtain $r_m - r_{BS}$ of about 0.8 fm, which is similar to the case of neutron-rich He isotopes. This leads to an interesting implication that such a difference is typical of nuclei having a neutron halo. In order to justify this implication, however, it is inevitable to confirm, by future experiments, the assumption that even for neutron-rich unstable nuclei, σ_R agrees with the black sphere cross section determined from the first peak angle in proton-nucleus elastic scattering differential cross section.

We acknowledge K. Yazaki for his invaluable suggestions and comments. We also acknowledge the members of Japan Charged-Particle Nuclear Reaction Data Group (JCPRG), especially N. Otuka, for kindly helping us collect the various data sets. K.I. thanks the Institute for Nuclear Theory at the University of Washington for its hospitality and the Department of Energy for partial support during the completion of this work. K.O. thanks Aichi Shukutoku University for its domestic research program, and Department of Physics at Nagoya University for its hospitality.

- [1] L. Ray, Phys. Rev. C **20**, 1857 (1979).
- [2] A. Kohama, K. Iida, and K. Oyamatsu, Phys. Rev. C **69**, 064316 (2004).
- [3] P.J. Karol, Phys. Rev. C **11**, 1203 (1975).
- [4] S. Kox *et al.*, Phys. Rev. C **35**, 1678 (1987).
- [5] L. Ray, G.W. Hoffmann, G.S. Blanpied, W.R. Coker, and R.P. Liljestrand, Phys. Rev. C **18**, 1756 (1978).
- [6] G.S. Blanpied *et al.*, Phys. Rev. Lett. **39**, 1447 (1977); Erratum *ibid.* **40**, 420 (1978).
- [7] G.S. Blanpied *et al.*, Phys. Rev. C **18**, 1436 (1978).
- [8] G.D. Alkhazov *et al.*, Nucl. Phys. **A381**, 430 (1982).
- [9] A. Chaumeaux, V. Layly, and R. Schaeffer, Phys. Lett. **72B**, 33 (1977).
- [10] L. Ray, Phys. Rev. C **19**, 1855 (1979).
- [11] G. Igo *et al.*, Phys. Lett. **81B**, 151 (1979).
- [12] G.D. Alkhazov *et al.*, Nucl. Phys. **A274**, 443 (1976).
- [13] G. Pauletta *et al.*, Phys. Lett. B **106**, 470 (1981).
- [14] H. de Vries, W. de Jager, and C. de Vries, At. Data Nucl. Data Tables **36**, 495 (1987).
- [15] G. Fricke *et al.*, At. Data Nucl. Data Tables **60**, 177 (1995).

- [16] The data have been retrieved from IAEA-NDS (International Atomic Energy Agency (IAEA)-Nuclear Data Service (NDS)) web site <http://www-nds.iaea.org/>
- [17] M. Geso *et al.*, Phys. Rev. C **65**, 034005 (2002).
- [18] R. Frascaria *et al.*, Nucl. Phys. **A264**, 445 (1976).
- [19] G.D. Alkhazov *et al.*, Phys. Lett. **85B**, 43 (1979).
- [20] H. Palevsky *et al.*, Phys. Rev. Lett. **18**, 1200 (1967).
- [21] G.D. Alkhazov *et al.*, JETP. Lett. **26**, 102 (1977).
- [22] S.D. Baker *et al.*, Phys. Rev. Lett. **32**, 839 (1974).
- [23] E. Aslanides *et al.*, Phys. Lett. **68B**, 221 (1977).
- [24] O.G. Grebenjuk *et al.*, Nucl. Phys. **A500**, 637 (1989).
- [25] G.S. Blanpied *et al.*, Phys. Rev. C **23**, 2599 (1981).
- [26] G.S. Blanpied *et al.*, Phys. Rev. C **32**, 2152 (1985).
- [27] G.D. Alkhazov *et al.*, Phys. Lett. **42B**, 121 (1972).
- [28] R. Bertini *et al.*, Phys. Lett. **45B**, 119 (1973).
- [29] G.S. Blanpied, M.L. Barlett, G.W. Hoffmann, and J.A. McGill, Phys. Rev. C **25**, 2550 (1982).
- [30] G.D. Alkhazov *et al.*, Report No. LNPI-531, Leningrad (1979).
- [31] G.S. Adams *et al.*, Phys. Rev. Lett. **43**, 421 (1979).
- [32] E. Bleszynski *et al.*, Phys. Rev. C **37**, 1527 (1988).
- [33] G.D. Alkhazov *et al.*, JETP. Lett. **28**, 662 (1978).
- [34] G.S. Blanpied *et al.*, Phys. Rev. C **30**, 1233 (1984).
- [35] G.S. Blanpied *et al.*, Phys. Rev. C **38**, 2180 (1988).
- [36] G.S. Blanpied *et al.*, Phys. Rev. C **20**, 1490 (1979).
- [37] G.S. Blanpied *et al.*, Phys. Rev. C **25**, 422 (1982).
- [38] G.S. Blanpied *et al.*, Phys. Rev. C **37**, 1987 (1988).
- [39] G.D. Alkhazov *et al.*, Sov. J. Nucl. Phys. **22**, 469 (1976).
- [40] G.D. Alkhazov *et al.*, JETP. Lett. **18**, 181 (1973).
- [41] E. Bleszynski *et al.*, Phys. Rev. C **25**, 2563 (1982).
- [42] L. Ray *et al.*, Phys. Rev. C **23**, 828 (1981).
- [43] M.A. Zhusupov, E.T. Ibraeva, Bulletin of the Russian Academy of Sciences, Physics, **60**, 809 (1996).
- [44] E. Friedman and A. Gal, Nucl. Phys. **A724**, 143 (2003).
- [45] G.F. Bertsch and R.A. Broglia, *Oscillations in Finite Quantum Systems* (Cambridge University Press, Cambridge, 1994).
- [46] W. Bauhoff, At. Data Nucl. Data Tables **35**, 429 (1986).
- [47] S. Eidelman *et al.*, Phys. Lett. B **592**, 1 (2004).
- [48] R. Arndt *et al.*, Phys. Rev. D **28**, 97 (1983).
- [49] M.M. Gazzaly *et al.*, Phys. Rev. C **25**, 408 (1982).
- [50] G.W. Hoffmann *et al.*, Phys. Rev. Lett. **40**, 1256 (1978).
- [51] A. Ozawa, T. Suzuki, and I. Tanihata, Nucl. Phys. **A693**, 32 (2001).
- [52] J. Jaros *et al.*, Phys. Rev. C **18**, 2273 (1978).
- [53] K. Iida, A. Kohama, and K. Oyamatsu (unpublished).
- [54] A. Kohama, K. Iida, and K. Oyamatsu (unpublished).
- [55] S.R. Neumaier *et al.*, Nucl. Phys. **A712**, 247 (2002).
- [56] G.D. Alkhazov *et al.*, Nucl. Phys. **A712**, 269 (2002).
- [57] I. Tanihata *et al.*, Phys. Lett. **287B**, 307 (1992).